

# Synthesis and characterization of amphiphilic block copolymers from poly(ethylene glycol)methyl ether and 4-methyl- $\epsilon$ -caprolactone or 4-phenyl- $\epsilon$ -caprolactone

Ren-Shen Lee <sup>a,\*</sup>, Chia-Bin Hung <sup>b</sup>

<sup>a</sup> Center of General Education, Chang Gung University, 259 Wen-Hwa 1st Road, Kwei-Shan, Tao-Yuan 333, Taiwan, ROC

<sup>b</sup> Department of Chemical Engineering and Materials, Chang Gung University, Tao-Yuan, Taiwan, ROC

Received 25 October 2006; received in revised form 28 February 2007; accepted 1 March 2007

Available online 12 March 2007

## Abstract

MPEG-*b*-PMCL and MPEG-*b*-PBCL diblock copolymers were synthesized by ring-opening polymerization of 4-methyl- $\epsilon$ -caprolactone (MCL) or 4-phenyl- $\epsilon$ -caprolactone (BCL) using monomethoxy poly(ethylene glycol) (MPEG,  $M_n = 550$  or  $2000 \text{ g mol}^{-1}$ ) as the macroinitiator and SnOct<sub>2</sub> as the catalyst. These copolymers were characterized by differential scanning calorimetry (DSC), <sup>1</sup>H NMR, <sup>13</sup>C NMR, and gel permeation chromatography. The thermal properties ( $T_g$  and  $T_m$ ) of the diblock copolymers depend on the composition of polymers. When larger amount of MCL or BCL was incorporated into the macromolecular backbone there was an increase in  $T_g$ . Their micellar characteristics in the aqueous phase were investigated by fluorescence spectroscopy, transmission electron microscopy (TEM), and dynamic light scattering (DLS). The block copolymers formed micelles in the aqueous phase with critical micelle concentrations (CMCs) in the range of 0.5–2.9  $\text{mg L}^{-1}$ , depending on the composition of polymers. The lengths of hydrophilic segment influence the shape of micelle. The mean hydrodynamic diameters of micelles from DLS were in the range of 70–140 nm. The drug entrapment efficiency and the drug-loading content of micelles depending on the composition of block polymers were described.

© 2007 Elsevier Ltd. All rights reserved.

**Keywords:** Amphiphilic; MPEG/PMCL or PBCL diblock copolymer; Critical micelle concentration

## 1. Introduction

Amphiphilic copolymers are well-known for self-assembly into micelles or larger aggregates in selective solvents for one block. In aqueous solutions, a core–shell structure is commonly formed, with a hydrophobic core surrounded by a hydrated hydrophilic shell. Desire to exploit the properties of block copolymer micelles in biomedical applications, namely the efficacious delivery of hydrophobic drugs sequestered within micellar cores, has more attention in biocompatible and biodegradable amphiphiles [1–5].

The poly(ethylene glycol) (PEG) block is known for biocompatibility [6], hydrophilicity, and water solubility at

moderate temperatures. Recently, poly(ethylene glycol)-*block*-poly( $\epsilon$ -caprolactone) (PEG-*b*-PCL) copolymers have been prepared by ring-opening polymerization of  $\epsilon$ -caprolactone ( $\epsilon$ -CL) using PEG as the macroinitiator [7–9]. The anionic coordination polymerization of  $\epsilon$ -CL can be initiated with hydroxyl end-capped PEG in the presence of either aluminum alkoxide [10,11] or tin octoate [12–15]. Tin carboxylate is actually a coinitiator to convert the hydroxyl end group into tin alkoxides. Methoxy poly(ethylene glycol) (MPEG) is a hydrophilic block, which has non-toxic components containing hydroxyl functional groups at one end of the chain, which can initiate the ring-opening polymerization of  $\epsilon$ -CL [16–18]. However, up to now, only a few references to the block polymerization of PEG with 4-methyl- $\epsilon$ -caprolactone (MCL) were reported. For example, Jérôme et al. [19,20] synthesized MPEG-*b*-PMCL by the ring-opening polymerization of MCL with MPEG in the presence of triethylaluminum

\* Corresponding author. Tel.: +886 3 2118800x5054; fax: +886 3 2118700.

E-mail address: [shen21@mail.cgu.edu.tw](mailto:shen21@mail.cgu.edu.tw) (R.-S. Lee).

as a catalyst and characterized in aqueous solution. Hillmyer et al. [21] studied the aqueous dispersions of block copolymers, MPEG-*b*-PMCL. Hedrick et al. [22] prepared PMCL containing highly branched block copolymers, with a molecular weight distribution higher than 1.7. Seefried and Koleske [23] measured the glass-transition temperatures of several methyl-substituted PCLs, and Deng et al. [24,25] studied on the ring-opening polymerization of 4-phenyl- $\epsilon$ -caprolactone and 6-phenyl- $\epsilon$ -caprolactone. To the best of our knowledge, methoxy poly(ethylene glycol)-*block*-poly(4-phenyl- $\epsilon$ -caprolactone) (MPEG-*b*-PBCL) diblock copolymers have never been investigated.

The aims of this work are thus to prepare diblock copolymers of MPEG-*b*-PMCL and MPEG-*b*-PBCL, and study the influence of hydrophilic/hydrophobic chain length of block copolymer on micelle size, drug entrapment efficiency, and drug-loading content. The physicochemical properties of these micelles in an aqueous phase were examined by fluorescence spectroscopy, dynamic light scattering (DLS), and transmission electron microscopy (TEM).

## 2. Experimental

### 2.1. Materials

MPEG 550 (MPEG12), 2000 g mol<sup>-1</sup> (MPEG45), 4-methylcyclohexanone, 4-phenylcyclohexanone, pyrene, amitriptyline hydrochloride (AM), and  $\epsilon$ -CL were purchased from Aldrich Chemical Co. (Milwaukee, WI). *m*-Chloroperoxybenzoic acid (*m*-CPBA) was purchased from Fluka Chemical Co. (Buchs SG1, Switzerland). Stannous octoate (SnOct<sub>2</sub>) was purchased from Strem Chemical Co. (Newburyport, MA). MPEG 550 and 2000 were dried over molecular sieves 4 Å (Acros, New Jersey, USA), and vacuum oven at 50 °C for overnight before use, respectively.  $\epsilon$ -CL was dried and vacuum distilled over calcium hydride (Merck, Darmstadt, Germany). MCL and BCL were prepared according to the reported method [19]. Organic solvents such as tetrahydrofuran (THF), methanol, chloroform, and *n*-hexane were of high

pressure liquid chromatography (HPLC) grade and were purchased from Merck Chemical Co. (Darmstadt, Germany). Ultrapure water was used by purifying with a Milli-Q Plus (Waters, Milford, MA).

### 2.2. Synthesis of MPEG-*b*-PMCL and MPEG-*b*-PBCL diblock copolymers

All glasses were dried by oven and handled under a dry nitrogen stream. The typical process for the polymerization to give MPEG45-*b*-PMCL40 is as follows. MPEG45 ( $M_n = 2000$  g mol<sup>-1</sup>) (0.9 g, 0.45 mmol) and MCL (2.57 g, 22.51 mmol) were introduced into a flask and heated under a dry nitrogen stream to dissolve MPEG45. Then, 52 mg of SnOct<sub>2</sub> (1.5 wt% based on the weight of MPEG and MCL) was administered into the flask. The flask was purged with nitrogen and reacted at 140 °C for 24 h. The resulting product was dissolved in CHCl<sub>3</sub> and then precipitated into excess *n*-hexane with stirring. The purified polymer was dried *in vacuo* at 50 °C for 24 h and then analyzed. The yield ranged between 73 and 97%. Representative <sup>1</sup>H NMR and <sup>13</sup>C NMR spectra of the MPEG45-*b*-PMCL40 are shown in Figs. 1 and 2.

### 2.3. Characterization

<sup>1</sup>H NMR and <sup>13</sup>C NMR spectra were recorded at 500 MHz (with a Bruker WB/DMX-500 spectrometer, Ettlingen, Germany) with chloroform ( $\delta$  7.24 or 76.9 ppm) as an internal standard in chloroform-*d* (CDCl<sub>3</sub>). A thermal analysis of the polymer was performed on a DuPont 9900 system that consisted of DSC (Newcastle, DE). The heating rate was 20 °C min<sup>-1</sup>.  $T_g$ s were read at the middle of the change in the heat capacity and were taken from the second heating scan after quick cooling. Number- and weight-average molecular weights ( $M_n$  and  $M_w$ , respectively) of the polymer were determined by a GPC system. It was carried out on a Jasco HPLC system equipped with a model PU-2031 refractive-index detector (Tokyo, Japan), and Jordi Gel DVB columns

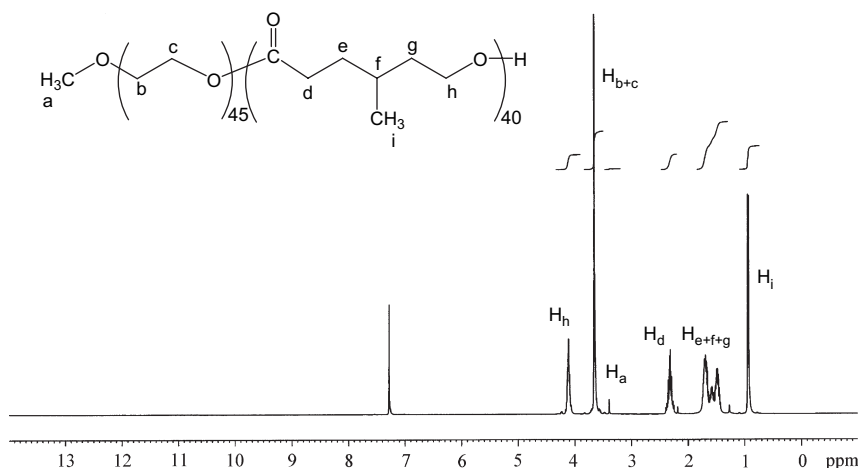


Fig. 1. Representative <sup>1</sup>H NMR spectrum of the MPEG45-*b*-PMCL40 diblock copolymer in CDCl<sub>3</sub>.

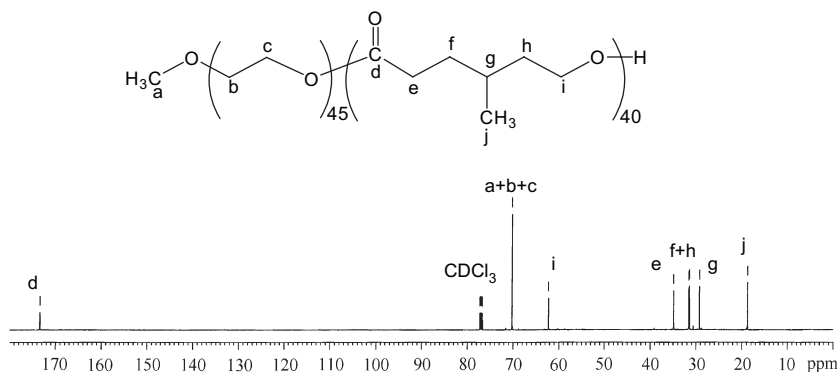


Fig. 2. Representative  $^{13}\text{C}$  NMR spectrum of the MPEG45-*b*-PMCL40 diblock copolymer in  $\text{CDCl}_3$ .

with pore sizes of  $10^2$ , 500, and  $10^3$  Å. Chloroform was used as an eluent at a flow rate of  $0.5 \text{ mL min}^{-1}$ . Polystyrene standards with a low dispersity (Polymer Sciences) were used to generate a calibration curve. Data were recorded and manipulated with a Windows-based software package (Scientific Information Service Co.).

UV–vis spectra were obtained using a Jasco V-550 spectrophotometer (Tokyo, Japan). The pyrene fluorescence spectra were recorded on a Hitachi F-4500 spectrofluorometer (Japan). Square quartz cells of  $1.0 \times 1.0 \text{ cm}$  were used. For fluorescence excitation spectra, the detection wavelength  $\lambda_{\text{em}}$  was set at 390 nm.

#### 2.4. Measurements of fluorescence spectroscopy

To prove the formation of the micelles, fluorescence measurements were carried out using pyrene as a probe [26]. Fluorescence spectra of pyrene in aqueous solution were recorded at room temperature on a fluorescence spectrophotometer. The sample solutions were prepared by first adding known amounts of pyrene in acetone to a series of flasks. After the acetone had evaporated completely, measured amounts of micelle solutions with various concentrations of MPEG45-*b*-PMCL40 (145, 72.5, and  $29 \text{ mg L}^{-1}$ ) were added to each of the flasks and mixed by vortexing. The concentration of pyrene in the final solutions was  $6.1 \times 10^{-7} \text{ M}$ . The flasks were allowed to stand overnight at room temperature to equilibrate the pyrene and the micelles. The emission wavelength was 390 nm for excitation spectra.

#### 2.5. Measurements of size and size distribution

The size distribution of micelles were estimated by a dynamic light scattering (DLS) using a Particle-Size Analyzer (Zetasizer nano ZS, Malvern, UK) at  $20^\circ\text{C}$ . The intensity of a scattered light was detected at  $90^\circ$  to an incident beam. Measurements were made after the aqueous micellar solution ( $C = 0.3 \text{ g L}^{-1}$ ) was filtered with a microfilter having an average pore size of  $0.2 \mu\text{m}$  (Advantec MFS, USA). An average size distribution of aqueous micellar solution was determined based on CONTIN programs of Provencher and Hendrix [27].

#### 2.6. Observation on transmission electron microscope

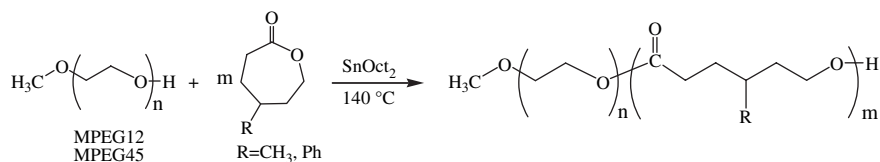
The morphology of the micelles was observed by TEM (JEM 1200-EXII, Tokyo, Japan). Drops of micelle solution ( $C = 0.3 \text{ g L}^{-1}$ ) were placed on a carbon film coated on a copper grid, and then were dried at room temperature. Observation was done at an accelerating voltage of 100 kV.

#### 2.7. Determination of drug-loading content and drug entrapment efficiency

Using oil-in-water solvent evaporation, MPEG-*b*-PMCL or MPEG-*b*-PBCL (10 mg) was dissolved in 6 mL methylene chloride followed by adding AM with various weight ratios to polymer (0.75/1–1.5/1) served as model drug. The solution was added dropwise to 150 mL distilled water containing 1 wt% poly(vinyl alcohol) under vigorous stirring. Poly(vinyl alcohol) was used as a surfactant to reduce the aggregation of micelle. Droplet size was reduced by sonication at ambient temperature for 60 min. The emulsion was stirred at ambient temperature for overnight to evaporate methylene chloride. The aggregated AM-loaded micelles were removed by centrifugation ( $3000 \text{ rpm} \times 30 \text{ min}$ ). Then, the aqueous micellar solution was dried at room temperature by vacuum rotary evaporator. The unloaded AM was eliminated by washing three times with distilled water because the solubility of AM in water is very large than that of block copolymer and micelle. The micelles were obtained by vacuum drying. A weighed amount of micelle was disrupted by the addition of acetonitrile (10 mL). Drug content was assayed spectrophotometrically at 240 nm using a Diode Array UV–vis Spectrophotometer. The drug-loading content and drug entrapment efficiency were calculated by Eqs. (1) and (2), respectively:

$$\text{Drug-loading content (\%)} = \left( \frac{\text{weight of drug in micelles}}{\text{weight of micelles}} \right) \times 100 \quad (1)$$

$$\begin{aligned} \text{Drug entrapment efficiency (\%)} \\ = \left( \frac{\text{weight of drug in micelles}}{\text{weight of drug fed initially}} \right) \times 100 \end{aligned} \quad (2)$$

Scheme 1. The synthesis of MPEG-*b*-PMCL and MPEG-*b*-PBCL diblock copolymers.

### 3. Results and discussion

#### 3.1. Synthesis and characterization of the MPEG-*b*-PMCL and MPEG-*b*-PBCL copolymers

Various amphiphilic MPEG-*b*-PMCL and MPEG-*b*-PBCL diblock copolymers were synthesized by ring-opening polymerization of either MCL or BCL with hydroxyl-terminated macroinitiators MPEGs containing the number-average molecular weight 550 and 2000 g mol<sup>-1</sup>. The synthesis of amphiphilic MPEG-*b*-PMCL and MPEG-*b*-PBCL block copolymers is illustrated in Scheme 1. The hydroxyl group of MPEG was used as the initiation site for the ring-opening polymerization of MCL or BCL in the presence of SnOct<sub>2</sub> (1.5 wt%) as the catalyst in bulk at 140 °C for 24 h. With the fixed macroinitiator, copolymers with different compositions were prepared by changing the comonomer MCL or BCL feed ratio. The results of the polymerization are compiled in Table 1. The yields between 73 and 97% were high. The 4-methyl or 4-phenyl substitution of ε-CL reduces the polymerization rate, as also observed for other substituted lactones [28,29], and prevents the parent polymer from

crystallizing.  $M_n$ s of the block copolymers obtained from the copolymerization of MCL (or BCL) and MPEG increased with the increase of the molar ratios of MCL (or BCL) to MPEG in feed. When the MPEG12 was used as the macroinitiator, the molar ratios of MCL (or BCL) to MPEG12 in feed increase from 30 to 90, the  $M_n$ s of the copolymer increase from 3600 to 11 670 g mol<sup>-1</sup> with  $M_w/M_n$  between 1.57 and 1.97, and from 6870 to 13 620 g mol<sup>-1</sup> with  $M_w/M_n$  between 1.43 and 1.69, respectively. Similarly, if the MPEG45 was used as the macroinitiator, the  $M_n$ s of the block copolymers increased with the increase of the molar ratios of MCL (or BCL) to MPEG45 in feed. The molar ratio of the compositions in the block copolymers was analyzed by <sup>1</sup>H NMR. The amounts of comonomer incorporated into the copolymer could be calculated from a comparison of integral area of the resonance peaks  $\delta = 0.95$  ppm of the methyl protons of PMCL or the resonance peaks  $\delta = 2.65$  ppm of the methine protons of PBCL, with the resonance peaks  $\delta = 3.35$  ppm of the terminal methoxy protons of MPEG. From the <sup>1</sup>H NMR analysis, the conversion of copolymerization of the monomers was lower than the corresponding feeds when higher the molar ratio of monomer in feed. This is probably that the substituted

Table 1  
Result of the block copolymerization of substituted ε-caprolactone initiated with methoxy poly(ethylene glycol) in bulk at 140 °C with 1.5 wt% SnOct<sub>2</sub> as the catalyst for 24 h

Copolymer	R for 4- <i>R</i> -ε-CL	[4- <i>R</i> -ε-CL]/[MPEG] molar ratio in the feed	[4- <i>R</i> -ε-CL]/[MPEG] molar ratio <sup>a</sup>	Yield (%)	$M_{n,\text{GPC}}^b$	$M_w/M_n^b$	$M_{n,\text{NMR}}^c$	$M_{n,\text{th}}^d$	$T_g^e$ (°C)	$T_{m1}^e$ (°C)	$T_{m2}^e$ (°C)
PEG12- <i>b</i> -PCL50	H	50/1	50/1	73	8850	1.67	6257	6257	-64	57	56
PEG12- <i>b</i> -PMCL41	CH <sub>3</sub>	30/1	41/1	91	3600	1.97	5798	4390	-63	15	
PEG12- <i>b</i> -PMCL48	CH <sub>3</sub>	50/1	48/1	89	5620	1.69	6694	6950	-62	5	
PEG12- <i>b</i> -PMCL72	CH <sub>3</sub>	70/1	72/1	74	6960	1.57	9766	9510	-62		
PEG12- <i>b</i> -PMCL77	CH <sub>3</sub>	90/1	77/1	83	11 670	1.87	10 406	12 070	-61		
PEG12- <i>b</i> -PBCL26	C <sub>6</sub> H <sub>5</sub>	30/1	26/1	94	6870	1.69	5494	6254	-5		
PEG12- <i>b</i> -PBCL51	C <sub>6</sub> H <sub>5</sub>	50/1	51/1	90	8500	1.65	10 050	10 057	1		
PEG12- <i>b</i> -PBCL54	C <sub>6</sub> H <sub>5</sub>	70/1	54/1	94	13 930	1.43	10 810	13 850	3		
PEG12- <i>b</i> -PBCL51	C <sub>6</sub> H <sub>5</sub>	90/1	51/1	97	13 620	1.59	10 247	17 650	4		
PEG45- <i>b</i> -PCL45	H	50/1	45/1	89	5580	2.00	7130	7707	-60	57	50
PEG45- <i>b</i> -PMCL18	CH <sub>3</sub>	30/1	18/1	92	4760	1.56	4304	5840	-60	50	
PEG45- <i>b</i> -PMCL40	CH <sub>3</sub>	50/1	40/1	97	5500	1.70	7120	8400	-62	50	
PEG45- <i>b</i> -PMCL53	CH <sub>3</sub>	70/1	53/1	83	7950	1.57	8784	10 960	-59	48	
PEG45- <i>b</i> -PMCL69	CH <sub>3</sub>	90/1	69/1	77	9120	1.73	10 832	13 520	-59	47	
PEG45- <i>b</i> -PBCL27	C <sub>6</sub> H <sub>5</sub>	30/1	27/1	81	5100	1.90	7134	7700	-20		
PEG45- <i>b</i> -PBCL51	C <sub>6</sub> H <sub>5</sub>	50/1	51/1	97	8800	1.84	11 690	11 507	-19		
PEG45- <i>b</i> -PBCL54	C <sub>6</sub> H <sub>5</sub>	70/1	54/1	90	9230	1.60	12 260	15 300	-14		
PEG45- <i>b</i> -PBCL51	C <sub>6</sub> H <sub>5</sub>	90/1	51/1	94	8570	1.63	11 697	19 100	-10		

<sup>a</sup> Determined by <sup>1</sup>H NMR spectroscopy.

<sup>b</sup> Determined by GPC.

<sup>c</sup> Determined by <sup>1</sup>H NMR spectroscopy of diblock copolymer.

<sup>d</sup>  $M_{n,\text{th}} = M_{n,\text{MPEG}} + M_{4-R-\epsilon\text{-CL}} \times [M]/[I]$  (where  $M_{n,\text{MPEG}}$  is the number-average molecular weight of MPEG,  $M_{4-R-\epsilon\text{-CL}}$  is the molecular weight of 4-*R*-ε-CL,  $[M]$  is the monomer molarity concentration, and  $[I]$  is the initiator molarity concentration).

<sup>e</sup> Determined from DSC thermograms.

lactones polymerize significantly slower than  $\epsilon$ -caprolactone and stems from some transesterification. For BCL copolymerization, as the molar ratio of [BCL]/[MPEG] in feed is above 50, a maximum limitation for polymerization was observed. It is suggested that the conjugative effect and the spatial hindrance of the phenyl group have a strong influence on the polymerization [24].

Typical  $^1\text{H}$  NMR spectra of the block copolymer MPEG45-*b*-PMCL40 with a molar ratio of [MCL]/[MPEG45] = 40 are shown in Fig. 1. The typical signals of the MPEG blocks are seen at  $\delta = 3.35$  ( $\text{H}_a$ , methoxy protons) and 3.65 ppm ( $\text{H}_{b+c}$ , methylene protons). The resonance peaks of PMCL blocks are shown at  $\delta = 0.95$  ( $\text{H}_i$ , methyl protons), 1.40–1.80 ( $\text{H}_{e+f+g}$ ,  $\text{C}_{3+5}$  methylene and  $\text{C}_4$  methine protons), and 2.30 ppm ( $\text{H}_d$ ,  $\text{C}_2$  methylene protons). The  $^{13}\text{C}$  NMR spectrum of MPEG45-*b*-PMCL40 diblock copolymer is shown in Fig. 2. The typical signal of the MPEG blocks is seen at  $\delta = 70$  ppm. The resonance peaks of PMCL blocks are shown at  $\delta = 18.8$  ( $\text{C}_j$ , the methyl carbon), 29.3 ( $\text{C}_g$ , the methine carbon), 31.5 ( $\text{C}_h$ , the methylene carbon), 31.6 ( $\text{C}_f$ , the methylene carbon), 34.9 ( $\text{C}_e$ , the methylene carbon), 62.3 ( $\text{C}_i$ , the methylene carbon), and 173.5 ppm ( $\text{C}_d$ , the ester carbonyl carbon).

The thermal behaviors of the block copolymers are shown in Table 1. According to DSC, fixing the length of the MPEG block ( $M_n = 550 \text{ g mol}^{-1}$ ) and increasing the length of PMCL (or PBCL) block, an increase in  $T_g$ s was observed.  $T_g$ s of MPEG-*b*-PMCL and MPEG-*b*-PBCL are higher than MPEG-*b*-PCL. This is due to the steric hindrance of MCL containing the methyl substituents (or BCL containing the phenyl substituents) that reduces the flexibility of backbone. When larger amounts of MCL (or BCL) were incorporated into the macromolecular backbone there was a slight increase in  $T_g$ . The copolymers of MPEG12-*b*-PMCL except the composition ratios of [MCL]/[MPEG12] below 48, and MPEG12-*b*-PBCL exhibited only  $T_g$ . Therefore, the copolymers were amorphous. In contrast, when the composition ratios of [MCL]/[MPEG12] is below 48, the copolymer exhibited a  $T_m$  which is lower than the MPEG12-*b*-PCL. All the same, if the  $M_n$  of the MPEG was fixed at  $2000 \text{ g mol}^{-1}$ , increased the length of PMCL (or PBCL) block,  $T_g$ s of MPEG45-*b*-PMCL (or MPEG45-*b*-PBCL) increased either. For MPEG45-*b*-PBCL copolymers exhibited only  $T_g$  that are amorphous. However, for MPEG45-*b*-PMCL copolymers are semicrystalline, giving a decreased  $T_m$  when the composition ratios of [MCL]/[MPEG45] increased.

Fig. 3 shows the typical GPC curves of diblock copolymers as compared with those of the original MPEG macroinitiator. The GPC traces show a unimodal distribution of the block copolymer and do not show the presence of any possible homopolymerized PMCL. In each block copolymer, the peak shifted toward a higher molecular weight region in comparison with the peak of the original MPEG macroinitiator, with little change in the molecular weight distribution. In all, these preliminary results showed that the block copolymerization of the hydroxyl group-terminated MPEG macroinitiator and MCL using  $\text{SnO}_2$  catalyst was successful under the experimental conditions used.

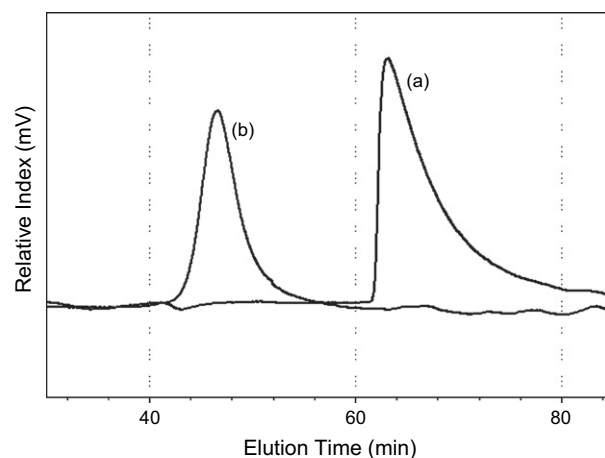


Fig. 3. GPC curves of (a) monohydroxyl end group MPEG45 macroinitiator and (b) MPEG45-*b*-PMCL40 diblock copolymer.

### 3.2. Micelles of block copolymers

The amphiphilic nature of the block copolymers, consisting of hydrophilic MPEG and hydrophobic PMCL (or PBCL) blocks, provides an opportunity to form micelles in water. The characteristics of the block copolymer micelles in an aqueous phase were investigated by fluorescence techniques. The critical micelle concentrations (CMCs) of the block copolymers in an aqueous phase were determined by a fluorescence technique using pyrene as a probe.

Excitation spectra of pyrene in the MPEG45-*b*-PMCL40 solution with various concentrations are shown in Fig. 4. As it can be seen, the fluorescence intensity increases with the increase in the concentration of MPEG45-*b*-PMCL40. The characteristic feature of pyrene excitation spectra, a red shift of the (0,0) band from 335 to 338 nm upon pyrene partition into micellar hydrophobic core, was utilized to determine the CMC values of MPEG-*b*-PMCL and MPEG-*b*-PBCL block copolymers. Fig. 5 shows the intensity ratios ( $I_{338}/I_{335}$ ) of pyrene excitation spectra versus the logarithm of MPEG12-*b*-PMCL48, MPEG45-*b*-PMCL69, MPEG45-*b*-PMCL40, MPEG45-*b*-PBCL51, and MPEG45-*b*-PCL45 block

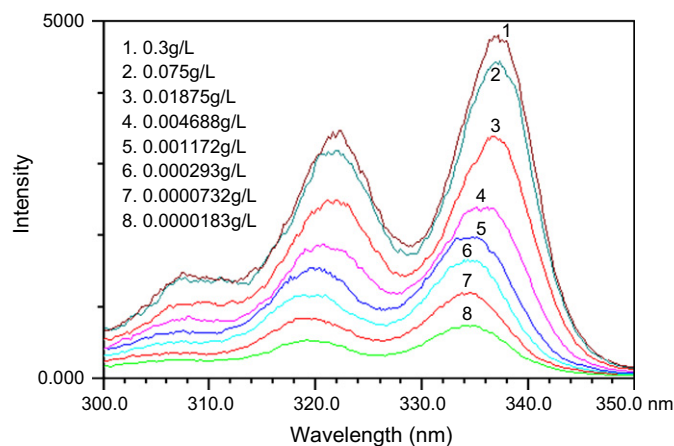


Fig. 4. Excitation spectra of the MPEG45-*b*-PMCL40 ([MCL]/[MPEG45] = 40/1) copolymer monitored at  $\lambda_{em} = 390 \text{ nm}$ .

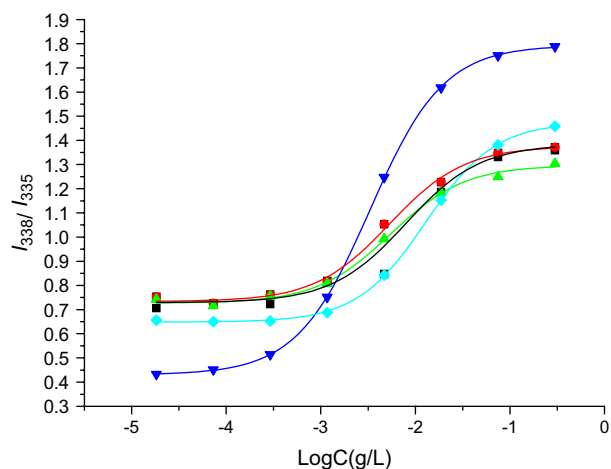


Fig. 5. Plot of the  $I_{338}/I_{335}$  intensity ratio (from pyrene excitation spectra; pyrene concentration =  $6.1 \times 10^{-7}$  M) versus the logarithm of the concentration (log C) for (■) MPEG12-*b*-PMCL48, (●) MPEG45-*b*-PMCL69, (▲) MPEG45-*b*-PMCL40, (▼) MPEG45-*b*-PBCL51, and (□) MPEG45-*b*-PCL45 diblock copolymers ( $\lambda_{em} = 390$  nm).

copolymers' concentration. The CMC was determined from the intersection of straight line segments, drawn through the points at the lowest polymer concentrations, which lie on a nearly horizontal line, with that going through the points on the rapidly rising part of the plot. The CMC values of the block copolymers depending on the block composition are shown in Table 2. At the fixed length of hydrophilic block (MPEG45), the sequences of CMC values of the block copolymers were MPEG45-*b*-PCL45 > MPEG45-*b*-PMCL40 > MPEG45-*b*-PMCL69 > MPEG45-*b*-PBCL51. The length and steric hindrance of hydrophobic segment increased and the CMC values decreased. The lower CMC values for MPEG-*b*-PMCL and MPEG-*b*-PBCL clearly show that introduction of hydrophobic methyl or phenyl group to the PCL makes self-association of block copolymers, thermodynamically, more favorable. As the length of hydrophilic (MPEG) segment increased, a reduced CMC values were observed. These results were in good agreement with those by other researches [16,30].

The mean hydrodynamic diameters of micelles from dynamic light scattering (DLS) were in the range of 70–140 nm, and size distribution showed a narrow and monodisperse unimodal pattern as shown in Figs. 6 and 7. Effect of polymer concentration on the size of micelles was observed

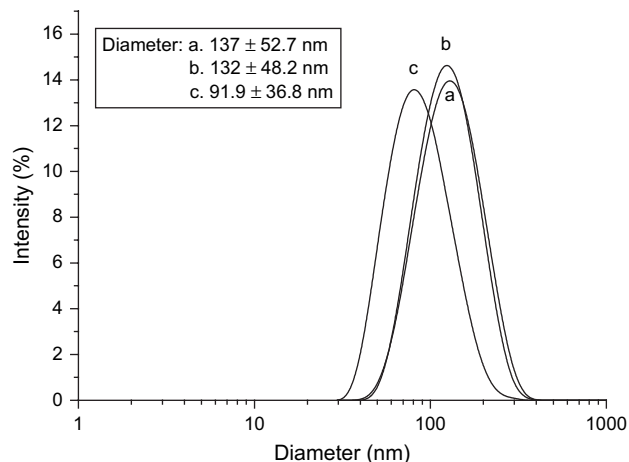


Fig. 6. Effect of MPEG12-*b*-PMCL48 concentration (a)  $145 \text{ mg L}^{-1}$ , (b)  $72.5 \text{ mg L}^{-1}$ , and (c)  $29 \text{ mg L}^{-1}$  on the size of micelle particles.

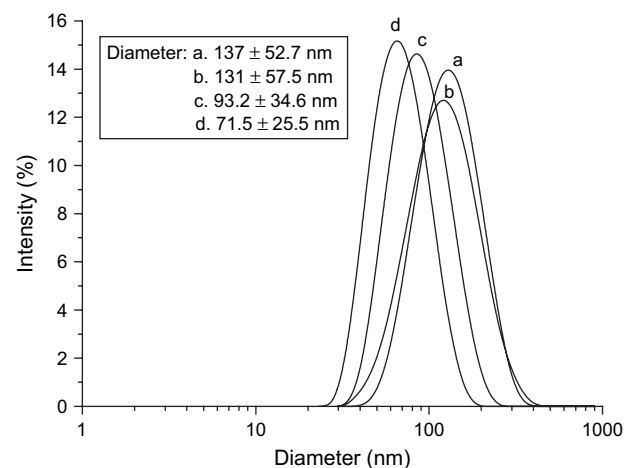


Fig. 7. Effect of the composition of copolymers (a) MPEG12-*b*-PMCL48, (b) MPEG45-*b*-PMCL69, (c) MPEG45-*b*-PBCL51, and (d) MPEG45-*b*-PMCL40 on the size of micelle particles at the 50-fold CMC ( $50 \times \text{CMC}$ ) value.

when increasing the concentration of MPEG12-*b*-PMCL48 from  $29 \text{ mg L}^{-1}$  ( $10 \times \text{CMC}$ ) to  $145 \text{ mg L}^{-1}$  ( $50 \times \text{CMC}$ ), the mean diameters of micelles increase from 92 to 137 nm [31]. Fixing the concentration at 50-fold CMC ( $50 \times \text{CMC}$ ) value, the size of micelles increases with the increase in the ratio of hydrophobic segment to the hydrophilic segment in copolymer. MPEG45-*b*-PMCL micelles were smaller than

Table 2  
Properties of AM-loaded MPEG-*b*-PM(B)CL diblock copolymer micelles<sup>a</sup>

Entry	Copolymer	CMC (mg/L)	Feed weight ratio (polymer/AM)	Drug entrapment efficiency (%)	Drug-loading content (%)	Micelle size (nm)
1	MPEG45- <i>b</i> -PMCL40	1.3	1/1.5	18.2	0.72	
2	MPEG45- <i>b</i> -PMCL40	1.3	1/1	23.6	0.89	$59.9 \pm 22.5$
3	MPEG45- <i>b</i> -PMCL40	1.3	1/0.75	9.4	0.20	
4	MPEG45- <i>b</i> -PMCL40	1.3	1/1	3.2	0.11	$76.9 \pm 31$
5	MPEG45- <i>b</i> -PCL45	2.4	1/1	53.3	2.09	
6	MPEG45- <i>b</i> -PBCL51	0.5	1/1	13.1	0.47	$131 \pm 44.5$
7	MPEG45- <i>b</i> -PMCL69	0.9	1/1	11.1	0.39	$97.8 \pm 42$
8	MPEG12- <i>b</i> -PMCL48	2.9	1/1	11.97	0.42	$62.9 \pm 15.5$

<sup>a</sup> The micelle formation at room temperature except the entry 4 at  $37^\circ\text{C}$ .

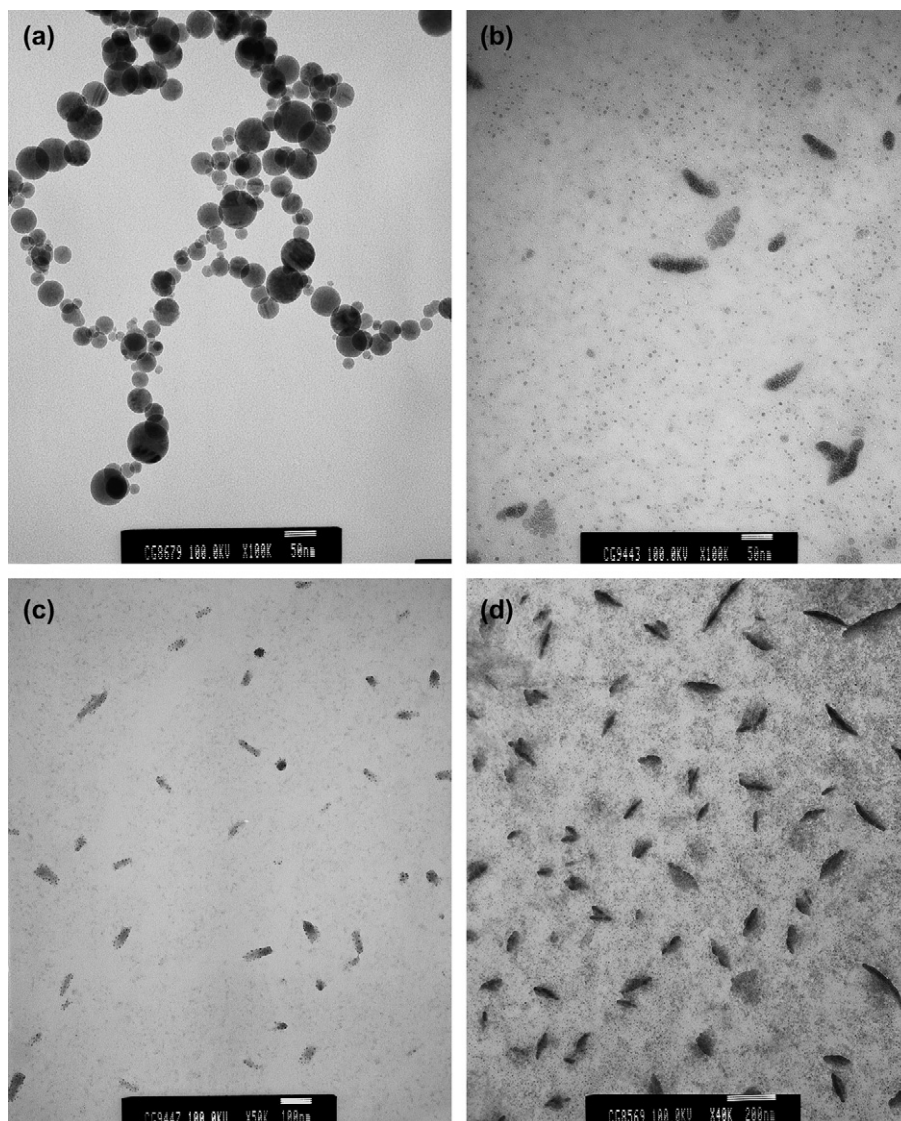


Fig. 8. TEM photograph of the micelles formed by (a) MPEG12-*b*-PMCL48, (b) MPEG45-*b*-PMCL40, (c) MPEG45-*b*-PMCL69, and (d) MPEG45-*b*-PBCL51.

MPEG12-*b*-PMCL micelle. These facts indicated that the micelles' size was dependent on the polymer concentration, the ratio of hydrophobic segment to hydrophilic segment, and the length of hydrophilic segment in the chain. Also, the morphology of the micelles is shown in Fig. 8. The lengths of hydrophilic segment influence the shape of micelle. The spindle shaped micelles with various lengths predominated for MPEG45-*b*-PMCL40, MPEG45-*b*-PMCL69, and MPEG45-*b*-PBCL51. The spherical shaped micelle that is similar to the PCL nanoparticles was observed only for MPEG12-*b*-PMCL48.

### 3.3. Drug-loading content and drug entrapment efficiency

An amount of AM incorporated into MPEG-*b*-PMCL and MPEG-*b*-PBCL micelles was calculated by the difference in weight ratio of AM in nanosphere to the preweight AM-loaded

micelles, which was calculated by UV absorbance after removing free AM and AM-bounded on the surface of micelles by sonication with distilled water. The amount of AM introduced into the micelle by controlling the weight ratio between polymer and drug is shown in Table 2. The drug entrapment efficiency and the drug-loading content increased with the weight ratio of drug to polymer. But if the feed weight ratio is increased over 1, a reduction in the drug entrapment efficiency and the drug-loading content was observed. A maximum drug entrapment efficiency and loading content was reached when the weight ratio is at 1/1. Also, the drug entrapment efficiency and the drug-loading content depending on the composition of block polymer were described. At the constant feed weight ratio (1/1), the drug entrapment efficiency and the drug-loading content increased with the increase in the length of hydrophilic segment (for MPEG12-*b*-PMCL48 and MPEG45-*b*-PMCL40) or with the decrease in the steric hindrance of hydrophobic segment (for MPEG45-*b*-PCL45,

MPEG45-*b*-PBCL51, and MPEG45-*b*-PMCL69). This due to have more steric hindrance hydrophobic segment in block copolymers, hinder the less amount of drug entrapped in micelles. As the micelle formation temperature increased from room temperature (25 °C) to 37 °C, the drug entrapment efficiency and the drug-loading content decreased remarkably due to the micelle formation that is less favor at 37 °C. Furthermore, the size of the AM-loaded polymer micelles is shown in Table 2. Compared the sizes of loaded and unloaded AM drug micelles, the size decreased when AM was loaded in MPEG-*b*-PMCL micelle. Contrarily, an increased micelle size was observed when AM was loaded in MPEG-*b*-PBCL micelle.

#### 4. Conclusion

Amphiphilic MPEG-*b*-PMCL and MPEG-*b*-PBCL diblock copolymers were successfully synthesized from MCL (or BCL) and MPEG as the macroinitiator. The molecular weight and unit compositions of the diblock copolymers were controlled by the molar ratios of MCL (or BCL) to the macroinitiator. CMC values were detected by fluorescence probe technique. An increase of the length and steric hindrance of hydrophobic segment in an amphiphilic diblock copolymer produced a lower CMC values. The drug entrapment efficiency and the drug-loading content increased with the length of hydrophilic block increased or the steric hindrance of hydrophobic block reduced. The morphology of the micelles exhibited a spindle or spherical shape depending on the length of hydrophilic block. Dynamic light scattering experiment showed that the mean hydrodynamic diameters of micelles were in the range of 70–140 nm. The drug release measurements are under way in our laboratory.

#### Acknowledgements

The research was supported by grants from National Science Council (NSC 95-2221-E-182-025) and Chang Gung University (BMRP123). The authors are grateful to Huang Shou-Ling and Kao Chung-Shen (Advanced Instrumentation Center, National Taiwan University) for obtaining <sup>13</sup>C NMR spectra and DSC measurement.

#### References

- [1] Kataoka K, Harada A, Nagasaki Y. *Adv Drug Delivery Rev* 2001;47:113.
- [2] Lavasanifar A, Samuel J, Kwon GS. *Adv Drug Delivery Rev* 2002;54:169.
- [3] Liggins RT, Burt HM. *Adv Drug Delivery Rev* 2002;54:191.
- [4] Bae Y, Fukushima S, Harada A, Kataoka K. *Angew Chem Int Ed* 2003;42:4640.
- [5] Riess G. *Prog Polym Sci* 2003;28:1107.
- [6] Allen C, Maysinger D, Eisenberg A. *Colloids Surf B* 1999;16:3.
- [7] Rashkov I, Espartero JL, Manolova N, Vert M. *Macromolecules* 1996;29:57.
- [8] He C, Sun J, Deng C, Zhao T, Deng M, Chen X, et al. *Biomacromolecules* 2004;5:2042.
- [9] Yuan M, Wang Y, Li X, Xiong C, Deng X. *Macromolecules* 2000;33:1613.
- [10] Duda A. *Macromolecules* 1996;29:1399.
- [11] Ropson N, Dubois P, Jérôme R, Teyssie P. *Macromolecules* 1995;28:7589.
- [12] Bogdanov B, Vidts A, Van Den Bulcke A, Verbeek R, Schacht E. *Polymer* 1998;39:1631.
- [13] Choi YK, Bae YH, Kim SW. *Macromolecules* 1998;31:8766.
- [14] Luo L, Tam J, Maysinger D, Eisenberg A. *Bioconjugate Chem* 2002;13:1259.
- [15] Storey RF, Sherman JW. *Macromolecules* 2002;35:1504.
- [16] Shim IG, Kim SY, Lee YM, Cho CS, Sung YK. *J Controlled Release* 1998;51:1.
- [17] Kim MS, Hyun H, Seo KS, Cho YH, Lee JW, Lee CR, et al. *J Polym Sci Part A Polym Chem* 2006;44:5413.
- [18] Kim MS, Hyun H, Cho YH, Seo KS, Jang WY, Kim SK, et al. *Polym Bull* 2005;55:149.
- [19] Vangeyte P, Jérôme R. *J Polym Sci Part A Polym Chem* 2006;44:1132.
- [20] Vangeyte P, Leyh B, Heinrich M, Grandjean J, Bourgaux C, Jérôme R. *Langmuir* 2004;20:8442.
- [21] Zupancich JA, Bates FS, Hillmyer MA. *Macromolecules* 2006;39:4286.
- [22] Trollsas M, Kelly MA, Claesson H, Siemens R, Hedrick JL. *Macromolecules* 1999;32:4917.
- [23] Seefried Jr CG, Koleske JV. *J Polym Sci Polym Phys Ed* 1975;13:851.
- [24] Deng X, Yuan M, Cao X, Li X. *Macromol Chem Phys* 2001;202:2417.
- [25] Yuan M, Li X, Liu Y, Deng X. *Macromol Chem Phys* 2001;202:546.
- [26] Wilhelm M, Zhao CL, Wang Y, Xu R, Winnik A. *Macromolecules* 1991;24:1033.
- [27] Provencher SW, Hendrix J. *J Phys Chem* 1978;69:4237.
- [28] Mecerreyes D, Miller RD, Hedrick JL, Detrembleur C, Jérôme R. *J Polym Sci Part A Polym Chem* 2000;38:870.
- [29] Parrish B, Quansah JK, Emrick T. *J Polym Sci Part A Polym Chem* 2002;40:1983.
- [30] Gao Z, Eisenberg A. *Macromolecules* 1993;26:7353.
- [31] Ge H, Hu Y, Jiang X, Cheng D, Yuan Y, Bi H, et al. *J Pharm Sci* 2002;91:1463.